Specific-heat measurements during cooling through the glass-transition region

M. Rajeswari and A. K. Raychaudhuri
Department of Physics, Indian Institute of Science, Bangalore 560012, India
(Received 17 October 1991; revised manuscript received 4 August 1992)

In this paper we report the measurements of specific heats of five glass formers as they are cooled through the glass-transition region. The measurements are compared with other specific-heat measurements such as adiabatic-calorimetry and ac-calorimetry measurements. The data are then analyzed using a model of enthalpy relaxation and nonequilibrium cooling, which can track the nonequilibrium relaxation time τ_s. The relevant parameters that describe τ_s are obtained, allowing us to compare the enthalpy-relaxation times obtained from this method with other methods. We display the clear connection of the unrelaxed enthalpy with the nonequilibrium relaxation time and also show the role played by the delayed heat release from the unrelaxed enthalpy in the glass-transition region. We have also made certain definite observations regarding the equilibrium configurational specific heat and the Vogel-Fulcher law, which describes τ_s.

I. INTRODUCTION

In this paper we report measurements and quantitative analysis of specific heats (C_p) of simple organic-glass-forming liquids as they are cooled through the glass transition region. For these measurements, we depart from commonly adopted adiabatic or differential scanning calorimetry for reasons mentioned below. Instead, we use the continuous cooling calorimetry[1] (a variation of relaxation calorimetry,[2,3]) which enables one to measure C_p during the actual cooling process. From the analysis of our data, using a simple model for enthalpy relaxation and nonequilibrium cooling, we were able to calculate all the relevant parameters that govern the enthalpy relaxation near the glass transition. This enabled us to compare our data of the enthalpy relaxation time (τ_s) with those obtained from other types of calorimetry (like ac specific heat) and also the shear relaxation time (τ_G) at $T \sim T_g$. In addition, we were able to make certain important observations regarding the equilibrium configurational specific heat, the stretch exponential β, and the so called "thermodynamic" transition point (T_0). (T_0 and β will be explained later on.)

This type of calorimetry, used by us, are uncommon in studies of glass transition. We would like to show that this form of calorimetry is a potent tool for quantitative analysis of the specific heat near the glass transition interval. In addition, this method allows us to do certain types of experiments that one cannot do using calorimetry, which measures the specific heat during warm up. We were led to this experiment by the observation that most of the specific-heat measurements near the glass transition have been made during reheating of a quenched glass. [There are notable exceptions like the frequently quoted work of Thomas and Park[5] on B_2O_3 (see Fig. 1) and the transient[6] and ac calorimetry.[7,8] In the last two techniques the measurements were done staying close to the thermal equilibrium.] In many cases the measurement during reheating is a necessity because a rapid cooling is needed to avoid crystallization. However, the measurement of specific heat during the actual freezing process has largely remained unattended to.

When the specific heat of a glass is measured during reheating (after quenching it initially), one starts from a "frozen" state, which has a thermal history built into it. As a result, any quantitative analysis of the specific-heat data[9] needs a prior knowledge of its thermal history. In contrast, in measurement during cooling, the starting state ($T_m > T > T_g$) is an equilibrium state in the sense that the enthalpy relaxation time (τ_s) is shorter than the experimental time scale (τ_{exp}). (The supercooled liquid state, however, is not a true equilibrium state if one considers the underlying crystalline state.) This makes the analysis simpler. In this case to describe the nonequilibrium cooling process one has to track down the liquid-like "excess," which slowly gets frozen, starting from a zero value. One clear manifestation of the difference between the C_p measured during heating and cooling can be seen in Fig. 1. While C_p measured during cooling decreases monotonically through T_g, the C_p measured dur-

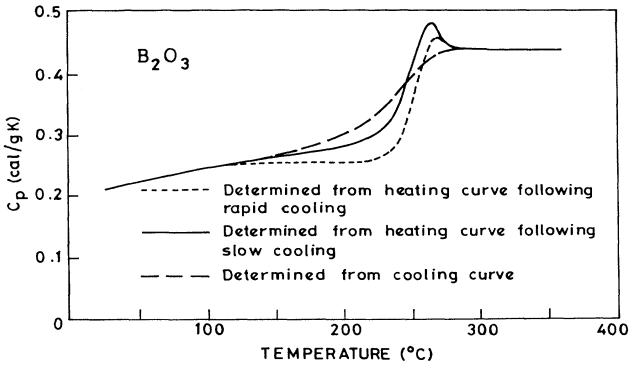

FIG. 1. Specific-heat measurement in B_2O_3 obtained during heating and cooling (data obtained from Ref. 5).

ing heating shows an overshoot. This overshoot is entirely of kinetic origin and contains information about the enthalpy lost during prior sub-T_g hold[10] and is sensitive to the thermal history.[9] This observed overshoot often complicates the shape of the C_p-T curve near T_g. We show in this paper that the shape of the C_p-T curve near T_g is very sensitive to the parameters governing the enthalpy relaxation, and using a relatively simple model we can obtain these parameters quantitatively from the cooling data.

The paper has five sections. The experimental details and results are given in Secs. II and III. In Sec. IV we present our model followed by an analysis of our data in Sec. V.

II. EXPERIMENTAL

The details of the measurement of specific heats during cooling are given elsewhere.[1,4,12] Here we present a short summary. This is essentially a modified form of thermal relaxation calorimetry.[2] Such a type of calorimetry has been used extensively in studies of time-dependent specific heats of glasses at low temperatures.[11] In this method the sample holder (a small copper cup of 1–2-ml volume sealed by an indium gasket) was thermally linked to a heat sink maintained at a constant temperature T_{bath} (see Fig. 2). T_{bath}, in our case, was the liquid-nitrogen temperature. The thermal characteristics of the link [i.e., heat leak rate $\dot{Q}(T)$] were determined experimentally. The sample held at $T > T_{\text{bath}}$, by applying power to a heater attached to the sample holder, was allowed to cool through the link by removing the heater power. As the sample cooled continuously through the link, loosing power $\dot{Q}(T)$, the temperature-time (T-t) curve was recorded. The heat capacity, $C(T)$, was obtained from the derivative $(dT/dt)_T$ of the cooling curve and the measured heat leak rate $\dot{Q}(T)$ using the following relation:

$$C(T)=\frac{\dot{Q}(T)}{(dT/dt)_T} . \tag{1}$$

The addenda heat capacity, determined in a separate run, was subtracted from the total heat capacity to obtain the sample heat capacity. The temperature was measured by a calibrated thermocouple or a diode. The entire experiment was automated using an IBM PC/XT compatible computer. To ensure that the bulk of the sample reached thermal equilibrium within the time scale of the experiment, a copper mesh was kept inside the sample copper cup. We also measured simultaneously the temperatures at the core of the sample and the outside of the copper cup to make sure that the bulk of the sample had attained thermal equilibrium. The absolute accuracy of our measurements, as well as the precision, was ~3%.

The heat capacity $C(T)$ obtained from Eq. (1) is the equilibrium heat capacity as long as it is time independent in the experimental time scale ($\tau_s \ll \tau_{\text{exp}}$). When $\tau_s \geq \tau_{\text{exp}}$, the $C(T)$ as defined in Eq. (1) is an "operational" heat capacity measured in the time scale τ_{exp}. This particular aspect, elaborated upon later on, is an important part of our analysis. The experimental time constant τ_{exp} is the RC time constant, where R is the effective thermal resistance to the bath [measured experimentally from $\dot{Q}(T)$] and C the total heat capacity.

Obtaining reproducible $C(T)$ data near the glass transition temperature need consistent thermal treatment during measurement. We followed the thermal treatment depicted in Fig. 3. The liquid was first quenched from T_i

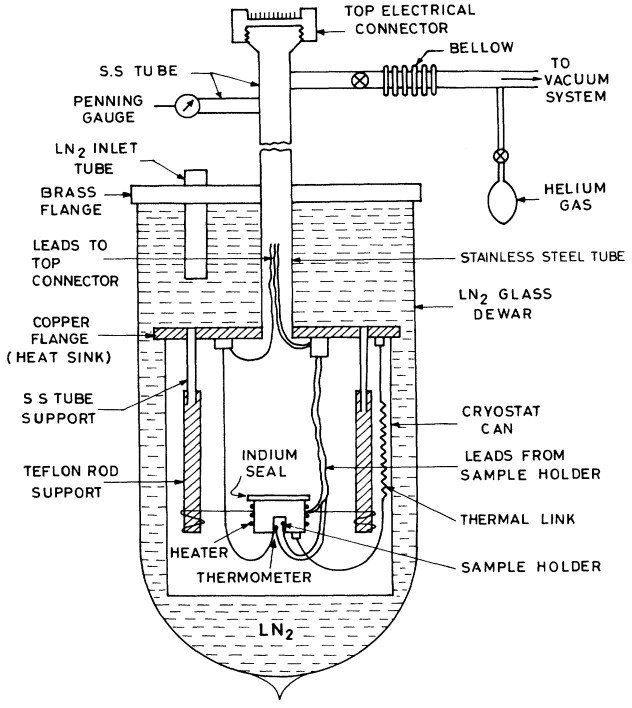

FIG. 2. Schematic of the experimental set up.

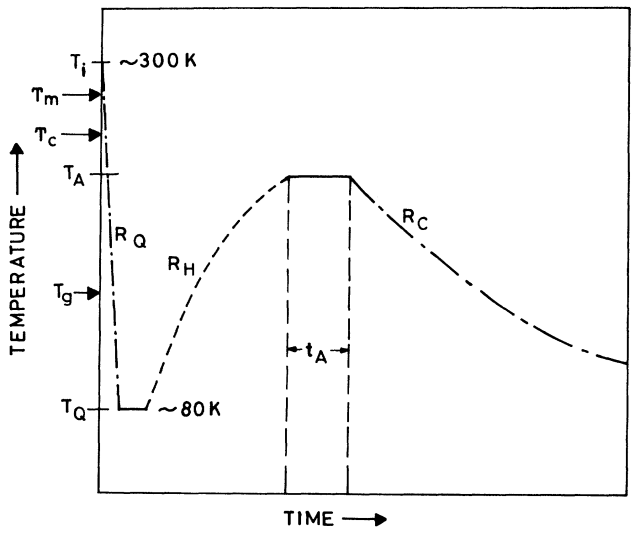

FIG. 3. Thermal treatment schedule followed in the measurement. The appropriate numbers are given in Table I and in the text. The heat capacity is measured after annealing at T_A, using the cooling curve marked R_c.

TABLE I. The details of the thermal treatment schedule followed in our experiment. For notations see the text; $T_i \approx 300$ K, $T_Q \approx 80$ K, $R_Q \approx 0.3$ K/sec and $t_A > 180$ min (see Fig. 3).

Material	T_A (K)	R_H (K/sec)	R_c (K/sec)
Glycerol	230	0.05	0.03
Propylene glycol	230	0.03	0.04
Amyl alcohol	170	0.07	0.02
Propylene carbonate	230	0.04	0.006
Diethyl phthalate	205	0.02	0.01

($T_i > T_m$, $T_i \approx 300$ K) to a temperature $T_Q \ll T_g$, at a rate R_Q (~ 0.25 K/s) by admitting helium exchange gas in the vacuum chamber. After evacuating the chamber to better than 10^{-5} torr, the sample was heated at a rate R_H (~ 0.05 K/s) to a temperature T_A such that $T_g < T_A < T_C$ (T_C is the temperature region where crystallization occurs on reheating). The supercooled liquid was then annealed at temperature T_A for a time t_A (> 3 h). The heater was then turned off and the sample was allowed to cool through the link to a temperature below T_g at an average rate R_C. It was during this slow cooling the (T-t) curves were recorded for the determination of $C(T)$. The relevant numbers for the thermal treatment of the liquids studied are given in Table I. Annealing of the sample at T_A is necessary to ensure that an equilibrium state is reached at the starting temperature. If the annealing time t_A is short, one finds anomalous features[12] appearing in $C(T)$ just below T_g.

Five materials with T_g lying in the range 120–190 K were used in this investigation (see Table II). The choice was governed by factors like suitable T_g (so that a range of temperature both above and below T_g can be scanned), availability, ease of handling, etc. Of these five materials, data from adiabatic calorimetry are available for three of them. Also, except propylene glycol, all the other materials can be crystallized in a controlled way, and their specific heats can be measured. In a separate report[13] we have discussed specific heats of partially crystallized supercooled liquids. All the samples were tested for impurities by gas chromatography. Any absorbed water was removed by heating the liquids at 120 °C for hours and then cooling and sealing them in a desiccator.

One of the materials, glycerol, may be the most studied glass former. It is classified as an "intermediate" liquid in terms of its temperature dependence of viscosity.[14] Another material, propylene carbonate, is a "fragile" liquid in terms of the same classification. We wanted to see if there is any qualitative difference in the temperature dependence of τ_s (the enthalpy relaxation time) of glycerol and propylene carbonate as $T \to T_g$. The other materials probably lie in between these in terms of "fragility."

III. RESULTS

In Fig. 4 we show the specific heats (C_p) of the five materials studied in the temperature range $1.3\ T_g > T > 0.8\ T_g$. In the same graph the data for the corresponding crystals are also shown. (Propylene glycol is the exception as it cannot be crystallized). We have also shown the data obtained from adiabatic calorimetry wherever available.[15–17] It can be seen that none of the specific heats obtained during cooling has the overshoot generally observed in the heating data. The adiabatic calorimetry data, obtained at a comparable or somewhat slower time scales than those used by us, show small but distinct overshoot in C_p occurring in the temperature range around T_g. For $T \gg T_g$ and $T \ll T_g$ the data obtained by both methods agree to within experimental accuracy. In the range $T \sim T_g$, $\tau_s \sim \tau_{\text{exp}}$ and the $C(T)$ data depends sensitively on τ_s, which, being a nonequilibrium relaxation time, depends on the details of thermal treatment and history. As a result, the shape of the $C(T)$ curve depends on the method of measurements. In Figs. 5 and 6 we show dC_p/dT for all the materials. In Fig. 5, d^2C_p/dT^2 for glycerol is also shown. We have taken the maximum in dC_p/dT (or the point, where d^2C_p/dT^2

TABLE II. The observed characteristics of the glass transition. The numbers in parentheses are from adiabatic calorimetry.

Material	Molecular weight	Melting point T_m (K)	Glass transition temperature T_g (K)	Width of transition ΔT_g (K)	Change in specific heat ΔC_p (J/gm K)
Glycerol	92	291	185 (180–190[a])	34 (19[a])	0.97 (0.91[a])
Propylene glycol	76		161 (155–165[b])	46 (18[b])	0.90 (0.94[b])
Amyl alcohol	88	191	123	30	0.72
Propylene carbonate	102	218	156	28	0.42
Diethyl phthalate	222	270	179 (175–185[c])	37 (20[c])	0.60 (0.55[c])

[a]Reference 15.
[b]Reference 16.
[c]Reference 17.

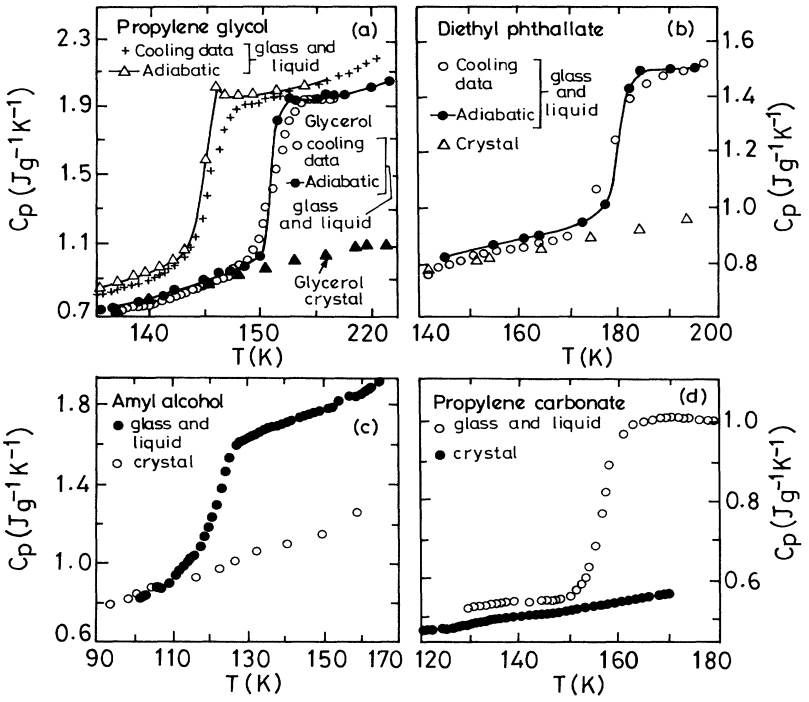

FIG. 4. Specific heat (C_p) data of the five materials studied. The data obtained by adiabatic calorimetry (Refs. 15–17) are also shown, as well as the data obtained on crystals.

crosses zero) as the glass transition temperature T_g. The glass transition interval is identified by temperatures T_U and T_L, where $d^2C_p/dT^2 \to 0$. This enables us to identify a width of the interval $\Delta T_g \equiv T_U - T_L$ and also the change in C_p at the glass transition, $\Delta C_p \equiv C_p(T_U) - C_p(T_L) \approx C_p(\text{liq}) - C_p$ (crystal). These quantities are shown in Table II.

The dC_p/dT for these materials show a small peak around $T/T_g \approx 0.9$. This extends the transition interval ΔT_g by about 15%–25%. Most likely this is due to secondary relaxation, although we have no definite explanation for it. This small peak does not affect our model calculation too significantly (see Sec. IV). However, it does limit the final accuracy of the parameters obtainable by the fit procedure.

For all the liquids studied $\Delta C_p/C_p(\text{liq}) \approx 0.4$–$0.5$. This is close to the same obtained from adiabatic calorimetry (see Table II). While the shape of the $C_p(T)$ curve at $T \sim T_g$ depends on the details of calorimetry the

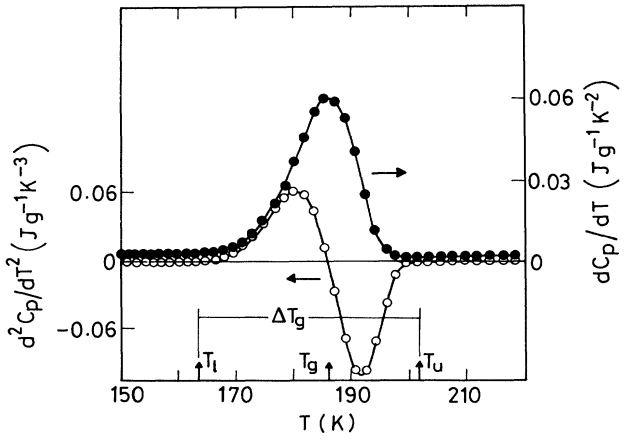

FIG. 5. The first (dC_p/dT) and second (d^2C_p/dT^2) derivatives of the observed specific heat of glycerol near the glass transition. The glass transition temperature T_g and the width of the transition $\Delta T_g = T_U - T_L$ are marked.

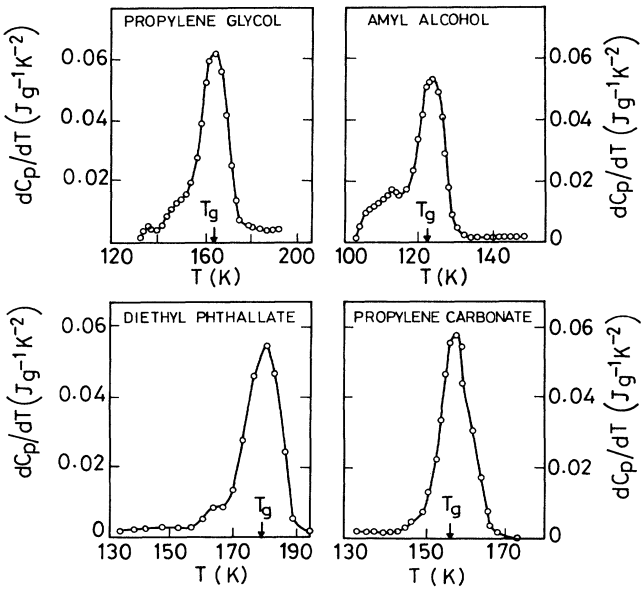

FIG. 6. The dC_p/dT for four materials near the glass transition. dC_p/dT is in the unit J/g K.[2] Please note the secondary peaks in dC_p/dT for these materials at around $T/T_g \approx 0.9$.

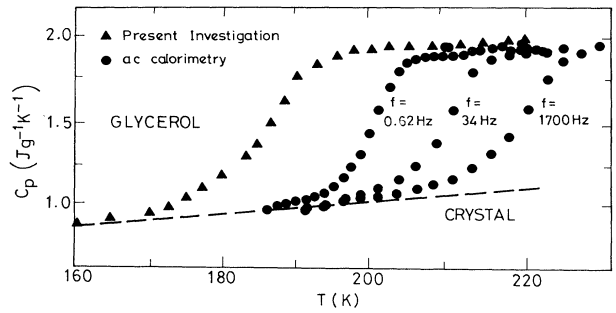

FIG. 7. Comparison of our data with ac specific-heat data (Ref. 7). The dashed line represents our data on crystals.

fractional change in specific heat is independent of these details. Our experiment and the adiabatic calorimetry were done on comparable time scales so that T_g observed by the two methods are also similar. We, however, find that the ΔT_g observed in adiabatic calorimetry are always smaller than those observed by us.

In Fig. 7 we have compared our experimental data on glycerol with those obtained from ac calorimetry.[7] The data taken by the two methods smoothly match at $T \gg T_g$. In our experiment the transition region is shifted to a much lower temperature because the $\tau_{\rm exp}$ is much larger, so that the effective frequency of measurement is much smaller. In both these methods data were taken during cooling, and no overshoot in the C_p is seen near the glass transition region.

The effective-time scale of our measurement ($\sim 10^3 - 4\times 10^3$ sec) is such that we can probe τ_s in the temperature range $T/T_g < 1.25$. This is the region of high viscosity.[14] In this range τ_s is determined by an activated process associated with a $(3N+1)$-dimensional potential energy surface.[18] As we will see later on, the continuity of enthalpy relaxation time without any change at $T/T_g \approx 1.25$ is distinct from what is observed in the shear relaxation time τ_a, which seems to have some kind of crossover at this temperature range, particularly for the fragile liquids.[14]

IV. THE MODEL OF ENTHALPY RELAXATION

In this section we present the model that has been used to analyze the cooling experiment and the specific-heat data. The enthalpy change of a supercooled liquid in response to a step change in T is given as

$$\Delta H(t) = \Delta H_L + \Delta H_R[1-\phi(t)] , \tag{2}$$

where ΔH_L represents the instantaneous contribution arising from the vibrational states (lattice modes) and ΔH_R is the relaxing part arising from the configurational states, which relax in a time scale τ_s. $\phi(t)$, the relaxation function, is given by the Williams-Watts function,[19]

$$\phi(t) = \exp[-(t/\tau_s)^{\beta}] , \tag{3}$$

where, $1 > \beta > 0$.

Following Eq. (2) we can define a time-dependent heat capacity

$$C_{\rm eff}(T,t) \equiv C_L(T) + C_{F0}(T)[1-\phi(t)] , \tag{4}$$

where C_L $(=\Delta H_L/\Delta T)$ is the solidlike vibrational heat capacity and C_{F0} $(=\Delta H_R/\Delta T)$ is the total equilibrium heat capacity associated with the configurational degrees of freedom. This is the excess liquidlike property, which is mostly removed, and the rest is frozen in as $T \to T_g$. In this model, the glass transition is a kinetic phenomena such that for $t/\tau_s \ll 1$, the response is solid like ($C_{\rm eff} \to C_L$), whereas for $t/\tau_s \gg 1$, the response is that of an equilibrium liquid ($C_{\rm eff} \to C_L + C_{F0}$).

If the cooling process is an equilibrium process, the observed enthalpy relaxation time is an equilibrium relaxation time $\tau_{\rm eq}$, i.e., $\tau_s \approx \tau_{\rm eq}$ when $\tau_s \ll \tau_{\rm exp}$. The equilibrium relaxation time is generally given by the Vogel-Fulcher equation,[20]

$$\tau_{\rm eq} = \tau_0 \exp\left[\frac{A}{(T-T_0)}\right] , \tag{5}$$

where, Ak_B is an activation energy and T_0 is a constant. Often a phase transition is postulated[21] at T_0 to resolve the Kauzmann paradox[22] because at $T \to T_0$ the excess entropy of the liquid seems to vanish. (It is for this reason we called T_0 the thermodynamic transition temperature.) In the actual cooling process $\tau_s \neq \tau_{\rm eq}$. The tracking of the nonequilibrium relaxation time is generally done by using the concept of fictive temperatures.[23-27] An alternative approach has been worked out by Kovacs.[28,29] Both these are, in the main, one-parameter models and are expected to be equivalent. The basic approach is to prevent τ_s from growing as fast as $\tau_{\rm eq}$ [Eq. (5)] as T_g is approached from above. For operational ease, we will use the approach of Kovacs. (We will show later on the equivalence of this approach and the fictive temperature approach.) The nonequilibrium aspect of τ_s is introduced through the relation,[28]

$$\tau_s = \tau_0 \exp\left[\frac{A}{(T-T_0)+A\delta}\right] . \tag{6}$$

The addition of the $A\delta$ term prevents τ_s from increasing as rapidly as $\tau_{\rm eq}$ while T is lowered through T_g. The time dependence arises through the time and temperature dependence of δ given by

$$\frac{d\delta}{dt} = -Dq - \delta/\tau_s . \tag{7}$$

Here, q is the cooling rate. D corresponds to fractional changes in the thermodynamic derivatives at T_g (e.g., the change in thermal expansion coefficient). For most glass formers it is expected to lie in the range 10^{-4}–10^{-6}. In our model we treated D as an adjustable parameter. At the starting point $T > T_g$ and $\tau_s \ll \tau_{\rm exp}$ so that $\tau_s \approx \tau_{\rm eq}$. This would imply $\delta = 0$. [When $\delta = 0$, Eq. (6) reduces to Eq. (5).] This shows the advantage of the cooling experiment that at the starting point $\tau_s \approx \tau_{\rm eq}$, and any frozen "excess," δ, is zero. On cooling δ starts developing nonzero values and τ_s starts deviating from $\tau_{\rm eq}$. (In cooling experiment $\tau_{\rm eq} > \tau_s$.)

The actual heat release from our sample is described by

the model shown schematically in Fig. 8. The effective heat capacity is expressed through Eq. (4). C_F is the time-dependent part and C_L is the instantaneous part. Both are connected to the bath (T_{bath}) through the link that leaks a power $\dot{Q}(T)$ and provides the cooling. In addition, there is an effective heat source Q^h present in the system, which arises due to the delayed heat release from the unrelaxed enthalpy of the system. We called this the "trapped heat."

To follow the cooling we approximate the continuous cooling process by a step cooling program in which the temperature steps ΔT are followed by isothermal holds of duration Δt such that $\Delta T = q \times \Delta t$, where q is the appropriate cooling rate at that temperature. As long as ΔT is not too large the exact step size is not important. To optimize the computational speed we used $\Delta t \approx 60$ sec, which corresponds to $\Delta T \lesssim 1$ K at $T \approx T_g$. Using the model of Fig. 8 we can write the ΔT of the nth cooling step (at $T = T_n$) as

$$\Delta T(T_n) = \frac{\Delta t[\dot{Q}(T_n) - \dot{Q}_n^r]}{C_{\text{eff}}(T_n, \Delta t)} . \quad (8)$$

In Eq. (8), the term $\dot{Q}_n^r$ is the rate of release of the trapped heat. The trapped heat Q_n^h (i.e., the total unrelaxed enthalpy at the beginning of the nth step) is calculated cumulatively by the relation,

$$Q_n^h = [C_{F0}(T_{n-1})\Delta T_{n-1} + Q_{n-1}^h]\phi(T_{n-1}, \Delta t) . \quad (9)$$

The first term is the unrelaxed enthalpy from the previous $(n-1)$th step and the second term is the cumulative unrelaxed enthalpy due to all prior steps. The amount of trapped heat released in the nth step is given by

$$\dot{Q}_n^r \Delta t = Q_n^r = Q_n^h[1 - \phi(T_n, \Delta t)] . \quad (10)$$

The delayed heat release associated with the unrelaxed enthalpy makes a significant contribution only near the glass transition.

From Eqs. (4) and (8)–(10) we can calculate the cooling rate (dT/dt) at $T = T_n$ and can obtain the heat capacity from Eq. (1) using experimentally observed $\dot{Q}(T_n)$. The nonequilibrium enthalpy relaxation time τ_s at each temperature is calculated from Eqs. (6) and (7). τ_s enters the calculation through the relaxation function $\phi(T_n, t)$ defined in Eq. (3). [For the calculation of δ in Eq. (7), we have replaced τ_s by τ_{eq}. This does not affect the results in any significant way but makes the calculation easier.] The calculated specific heat in subsequent discussions are referred to as $C_{\text{model}}(T)$.

In calculation of the specific heat we use C_{F0}, β, A, T_0, D, and δ as fit parameters. C_L is taken as the heat capacity of the crystal. The calculated heat capacity $C_{\text{model}}(T)$ is sensitive to these parameters in the region of glass transition. We optimize the parameters so that $C_{\text{model}}(T)$ and the observed specific heat agree to within 3–7%. The experimental "noise" is around 3%. An example of fit is shown in Fig. 9(a) for glycerol. While data of higher precision are definitely desirable to narrow down the range of parameter space, which gives the best fit, even with our data we find that the parameters can be identified within a narrow range (see Table III). The operational details of the calculation are given elsewhere[4] in order to keep the report in manageable size.

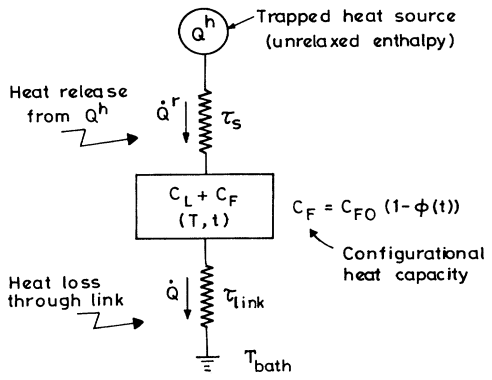

FIG. 8. Schematic representation of the model used for analyzing the data (see text for details).

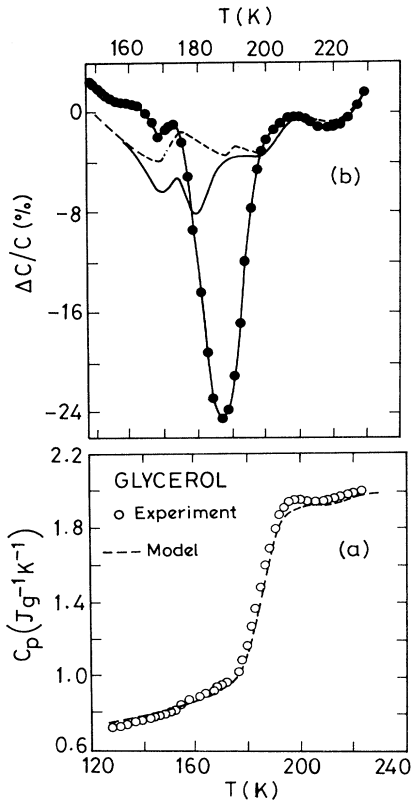

FIG. 9. Comparison of the observed and the calculated specific heats of glycerol. In (a) the data (○) and the calculated (— — —) values are shown. In (b) the relative error $\Delta C/C = (C_{\text{model}} - C_p)/C_p$ is shown as a function of T. The (— — —) curve represents the error in the best fit. The (——) curve represents the error when τ_{eq} is used for τ_s. The (—·—·—·) curve represents the error when the trapped heat release ($\dot{Q}^r$) is neglected.

TABLE III. The parameters of the model derived from the fit (see text).

Material	A (K)	τ_0 (sec)	T_0[a] (K)	D (K^{-1})	C_{F0}[b] (J/gm K)	β
Glycerol	2500±100	$(0.3-2)\times10^{-15}$	128–120	$(6\pm0.5)\times10^{-5}$	0.86–0.98	0.55±0.05
Propylene glycol	2170±100	$(0.1-5)\times10^{-14}$	112–100	$(3.8\pm0.5)\times10^{-5}$	0.80–0.93	0.45±0.05
Amyl alcohol	1700±50	$(0.3-3)\times10^{-14}$	83–81	$(1.0\pm0.3)\times10^{-5}$	0.50–0.70	0.50±0.02
Propylene carbonate	2200±100	$(0.2-1)\times10^{-15}$	114–90	$(0.1\pm.02)\times10^{-5}$	0.34–0.52	1.00±0.05
Diethyl phthalate	2300±100	$(0.2-1)\times10^{-15}$	119–100	$(3.0\pm0.5)\times10^{-5}$	0.54–0.57	0.70±0.03

[a]This is the range of variation of T_0 in the temperature range $1.25 > T/T_g > 0.85$.
[b]This is the range of variation of C_{F0} in the same temperature range.

The extent of sensitivity to fit parameters can be checked by varying an individual parameter around the best fit value. For instance, when the activation energy A is decreased by 20%, the $C_{\text{model}}(T)$ near the transition region differs from the observed value by about 15%. When τ_0 is changed by one order, the error increases to nearly 7%. Changing b by a factor of 2 can increase the error in the transition region as well as in the supercooled liquid region to more than 10%. The effect of varying relaxational parameters in the range $T < T_g$ is very small. The calculated heat capacity is most sensitive to these parameters in the transition ($T \sim T_g$) and in supercooled liquid ($T \gtrsim T_g$) region. The effect of using τ_{eq} instead of τ_s is shown in Fig. 9(b). The error encountered is small because we stay close to equilibrium. However, the effect of neglecting the delayed heat release [see Fig. 9(b)] can be large, and it does make a significant contribution in the region $T \sim T_g$.

The parameters obtained from our data for all the materials using the model are shown in Table III. In the following section we discuss the importance of these numbers and the related issues.

V. ANALYSIS OF THE DATA

A. Trapped heat [$Q^h(T)$] and the trapped heat release

The unrelaxed enthalpy (the trapped heat) cumulatively accumulates in the system as soon as τ_s becomes comparable to τ_{exp} in the cooling process. A part of this unrelaxed enthalpy is released subsequently. This acts as a heat source with a rate of power input $\dot{Q}^r(T)$ into the system. $Q^h(T)$ increases continuously as T is lowered. The $Q^h(T)$ calculated from our data using Eq. (9) are shown in Fig. 10. In the inset we show the rate of trapped heat release [$\dot{Q}^r(T)$] calculated from our model. While $Q^h(T)$ increases monotonically below T_g, $\dot{Q}^r(T)$ shows a maximum around $T/T_g \approx 1.03-0.97$. [For the other materials $\dot{Q}^r(T)$'s are similar to that of glycerol.] When $T > T_g$ and $\tau_s(T) \ll \tau_{\text{exp}}$ and $Q^h(T) \approx 0$ as a result $\dot{Q}^r(T) \approx 0$. When $T < T_g$ and $\tau_s(T) \gg \tau_{\text{exp}}$, $Q^h(T)$ is finite and monotonically increasing with decreasing T but $\dot{Q}^r(T)$ is again small because $\phi(t) \approx 1$. As a result, only at $T/T_g \approx 1$, $\dot{Q}^r(T)$ is finite and it shows a maximum.

The unrelaxed enthalpy is the liquidlike excess frozen into the system and, we will show later on, is closely related to δ [see Eqs. (6) and (7)], which tracks the nonequilibrium relaxation time τ_s. Using the definition of the fictive temperature (T_F) it can be shown that the unrelaxed enthalpy $Q^h(T)$ is directly related to T_F by the relation,[23,24]

$$Q^h(T) = H(T) - H_{\text{eq}}(T) = H_{\text{eq}}(T_F) - H_{\text{eq}}(T) \approx C_{F0}(T_F - T) , \quad (11)$$

where $H_{\text{eq}}(T)$ stands for the equilibrium enthalpy of the supercooled liquid at temperature T and C_{F0} is approximately taken as a constant. C_{F0} being known from the experiment, T_F can be calculated from $Q^h(T)$ directly. At $T > T_g$, $T_F \approx T$ and $Q^h \approx 0$. At $T \ll T_g$, $T_F \approx$ const, and as a result Q^h rises almost linearly as T is decreased, pro-

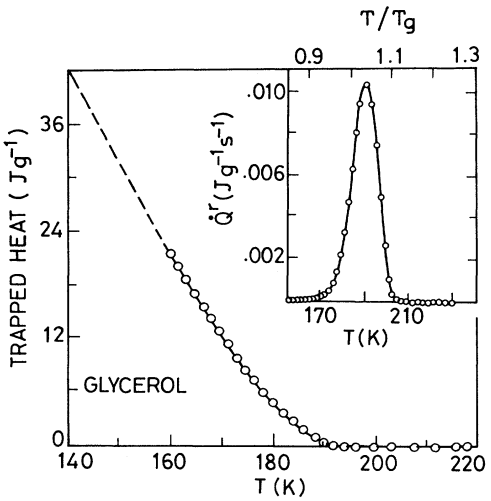

FIG. 10. The unrelaxed enthalpy (which we called the trapped heat) $Q^h(T)$ as obtained from our data using the model shown in Fig. 8. The inset shows the rate of delayed relaxation of this trapped heat $\dot{Q}^r(T)$. The dashed line shows the almost linear extrapolation following Eq. (11).

vided $C_{F0} \approx$ const. This has been shown in Fig. 10 as a broken line. In the next section we will discuss the role of $Q^h(T)$ and T_F in the determination of the nonequilibrium relaxation time τ_s.

B. The nonequilibrium relaxation time

The nonequilibrium relaxation time τ_s was calculated from the δ [Eqs. (6) and (7)]. The development of δ for glycerol, as T is lowered, is shown in Fig. 11. δ represents certain normalized unrelaxed liquid like "excess" (e.g., volume, enthalpy, etc.), which is both time and temperature dependent and remains frozen in. A comparison of Figs. 10 and 11 show the close similarity of Q^h and δ.

At $T < T_g$, it can be seen from Eq. (7) that $d\delta/dT \approx -D$. As a result δ (like Q^h) rises linearly with T as T is decreased. At any temperature one would expect that $Q^h/C_{F0} \approx \delta/D$. We find that such is indeed the case from our experimental data. δ has been determined from τ_s and Q^h has been determined independently from the cumulative accounting of the unrelaxed enthalpy. It is gratifying that these two quantities show the expected behavior. In the following we will see if the experimentally observed τ_s can be calculated from the T_F. The nonequilibrium relaxation time τ_s and the equilibrium relaxation time τ_{eq} [calculated from Eq. (5) using the parameters given in Table III] are shown in Fig. 12. The inset shows the fictive temperature. It can be seen that the glass transition occurs when $\tau_s \approx \tau_{exp}$. Also when $\tau_s > \tau_{exp}$ it starts to deviate from the τ_{eq}. In the same graph we have shown the τ_s obtained from the following Eq., which has been suggested from the Adam and Gibbs theory.[21,26,27] The τ_s in this theory is given as

$$\tau_s = \tau_0 \exp\left[\frac{B}{T \ln(T_F/T_0)}\right] . \tag{12}$$

Here we used B as an adjustable parameter, while others are used from Table III. We can see that the above relation cannot explain the observed τ_s. In particular, it

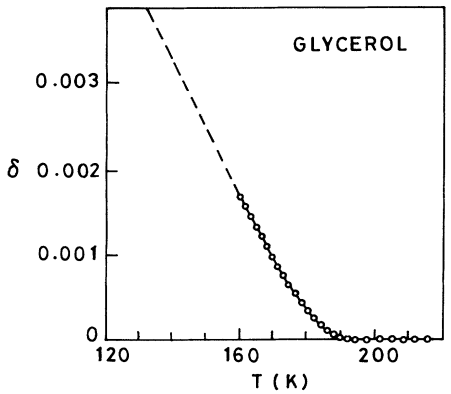

FIG. 11. The temperature variation of the parameter δ [see Eq. (6)], as obtained from the nonequilibrium relaxation time τ_s. The dashed line is the linear extrapolation [using Eq. (7)] when $\tau_s \gg \tau_{exp}$.

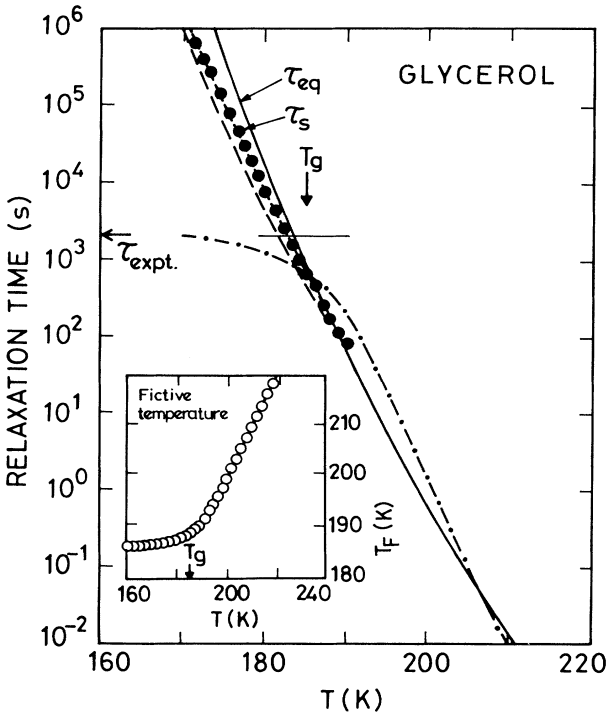

FIG. 12. The equilibrium relaxation time τ_{eq} [calculated from parameters of Table III using Eq. (5)] and the nonequilibrium relaxation time τ_s obtained in the experiment. The inset shows the fictive temperature T_F. The dashed-dotted curve represents the τ_s obtained from Eq. (12) and the dashed curve represents the τ_s obtained from Eq. (13). τ_{exp}, the experimental time scale is also marked.

severely overestimates the effect of nonequilibrium cooling.

We have also calculated τ_s using the following modified form of the Narayanaswamy equation:[24]

$$\tau_s = \tau_0 \exp\left[\frac{xA}{(T-T_0)} + \frac{(1-x)A}{(T_F-T_0)}\right] , \tag{13}$$

where $1 > x > 0$, and its depends on the cooling rate.[4] (It is higher for lower cooling rate.) The calculated τ_s is shown in Fig. 12 and was obtained with $x \approx 0.79$. The other parameters were the same as in Table III. We find that τ_s calculated from Eq. (13) agree well with the observed values. The τ_s in our experiment was generated from Eqs. (6) and (7) to make the $C_{model}(T)$ agree with the data. The fictive temperature used in calculation of τ_s from Eq. (13) was obtained independently from Q^h. The fact that the two independent approaches give the same τ_s, show their essential equivalence.

C. The equilibrium configurational specific heat C_{F0}

This is the complete contribution to the specific heat from all the configurational degrees of freedom that give an excess specific heat to the liquid. At $T \gg T_g$, the observed configurational specific heat $C_F \approx C_{F0}$ [see Eq. (4)].

At $T<T_g$, $C_F<C_{F0}$ and $C_F \rightarrow C_{F0}$ only in the limit $\tau_s/\tau_{exp} \rightarrow 0$. Our analysis of the data using the model allows us to find $C_{F0}(T)$ down to $T/T_g \approx 0.85$. (The low-temperature limit is decided by the experimental resolution. We generally stop at the temperature when $C_F/C_L \approx 3\%$, which is our precision). We find that C_{F0} rises as T decreases and approximately follows a relation $C_{F0} \approx C_0 + b/T$. We show this in Fig. 13 for glycerol along with the observed configurational specific heat C_F [$=C_p$ (observed) $-C_p$ (crystal)].

At $T \gg T_g$, $C_F \approx C_{F0}$, as expected. At around $T/T_g \approx 1.05$, the two start to differ. Our observation shows clearly that the observed fall of the specific heat at the glass transition is completely relaxational in origin. The actual thermodynamic configurational specific heat does not fall at $T \sim T_g$. On the contrary it keeps on rising at least till $T/T_g \approx 0.85$. This is a general observation, and we have seen this in all the materials studied. If the rise in C_{F0} is the signature of the onset of a phase transition[30] it must be occurring below $T/T_g \sim 0.85$. The rise in specific heat at lower T may also mean the tail of a Schottky contribution coming from two-level systems. However, the C_{F0} cannot rise like that at much lower temperatures. The question remains at what temperature the down turn occurs. In any case it will occur below $T/T_g \approx 0.8$. The observation about the temperature dependence of C_{F0} is an important issue and it definitely shows that the observed fall of the specific heat at T_g is completely due to relaxational effects (i.e., $\tau_s > \tau_{exp}$).

D. The thermodynamic transition temperature T_0

The equilibrium enthalpy relaxation time τ_{eq} as well as the nonequilibrium relaxation time τ_s are governed by the temperature T_0 [Eq. (5) and (6)]. T_0 is supposed to represent a true phase transition,[21,30] which is frustrated by diverging relaxation times. Assigning a thermodynamic meaning to T_0 brings in certain problems. We find that in all the materials studied and in the temperature range $T/T_g < 1.2$, T_0 is no longer a fixed quantity. If we want that the τ_s be given by Eq. (6), it is necessary that T_0 is decreased, though by a small amount, as T decreases. The extent of decrease varies from material to material. These are shown as a range of values for T_0 in Table III. Typical decrease is in the range 7–10 %. It is highest ($\sim$24%) for the most fragile liquid propylene carbonate. This observation that T_0 is not a constant, raises doubt about the universality of the Vogel-Fulcher equation [Eq. (5)]. (We raise this doubt with caution, yet with confidence because this equation has been used extensively in the field of glass transition.) The necessity of lowering of T_0 can be seen from our data. In Fig. 14, we show our data along with the calculated specific heat assuming $T_0 =$ constant. We cannot produce agreement between the observed and the calculated specific heats as long as we keep T_0 a constant.

The lowering of T_0 implies a "softening" of the divergence of τ_s and τ_{eq} as T is lowered. However, in the enthalpy relaxation times we do not see any change over to the Arrhenius behavior ($T_0 \rightarrow 0$) as we approach T_g, unlike that often observed in the shear relaxation time τ_G. In Fig. 15 we show the comparison of the τ_{eq} as obtained from our experiment and those obtained from other experiments. For glycerol, and "intermediate" liquid, our data match with those obtained by other methods in the region of overlap. (The data on glycerol are obtained from techniques, which include ac calorimetry, dielectric, and ultrasonic relaxations and digital correlation spectroscopy.[31] The longer time scale of our experiment allows us to extend the measurements to lower temperatures. In contrast, we find that for fragile liquid propylene carbonate, the temperature dependence of τ_{eq} as seen from the enthalpy relaxation is markedly different from those seen by other techniques.[32] We do not observe the changeover to the Arrhenius behavior. Similar conclusion had been reached on enthalpy relaxation time of another fragile liquid O-terphenyl mixtures from ac

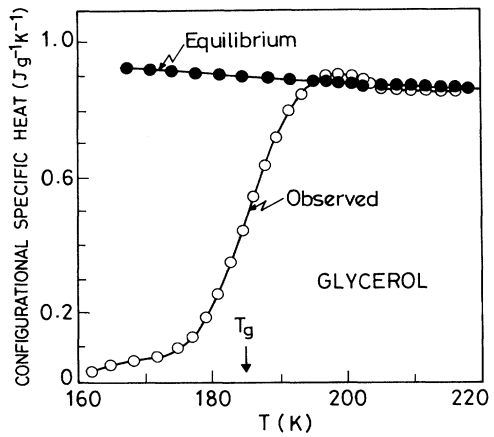

FIG. 13. The equilibrium configurational specific heat (C_{F0}) and the observed configurational specific heat (C_F) for glycerol [see Fig. 8 and Eq. (4)]. Note that C_{F0} continues to rise below T_g, while the observed C_F shows a fall due to relaxation effects.

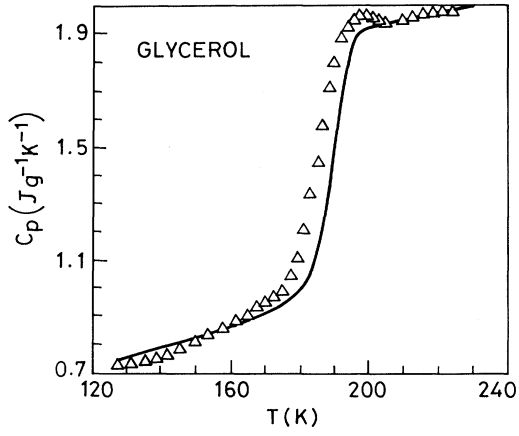

FIG. 14. The observed specific heat (C_p) and the calculated specific heat (solid line) taking T_0 as a constant in Eq. (6). For best fit, T_0 has to be decreased slightly as T is lowered. (See Table III.)

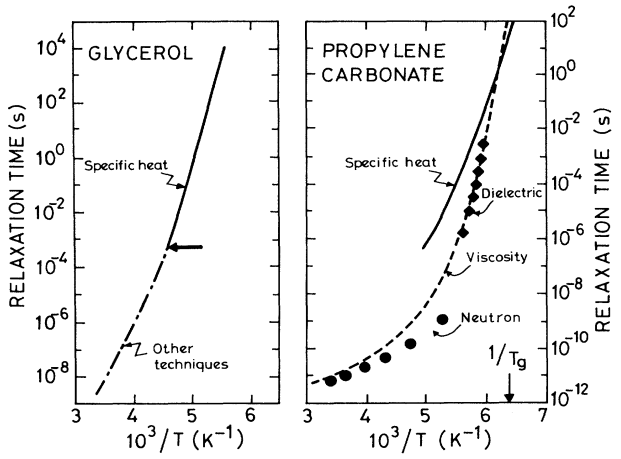

FIG. 15. The equilibrium enthalpy relaxation times (τ_{eq}) for glycerol and propylene carbonate as obtained from the present investigation (——) (see Table III). These are compared with those obtained from other techniques. For glycerol (—·—·—·) the data are obtained from Ref. 31. For propylene carbonate (— — —) the data are obtained from Ref. 32. The arrow in the data for glycerol shows the point where the enthalpy relaxation data of Ref. 7 merge with those of the present investigation.

calorimetry experiments.[8] Taking into consideration both these enthalpy relaxation data it seems that the strong fragility seen in shear relaxation time is not observed in the enthalpy relaxation time. At the same time one observes a small but continuous decrease in T_0 at lower temperatures leading to a softening of the divergence of τ_{eq}.

E. The exponent β

The parameter β in the relaxation function [Eq. (3)], have been evaluated for the liquids investigated and are given in Table III. For the aliphatic alcohols $\beta \approx 0.45-0.55$, whereas for the aromatic esters, β is closer to 1 and in propylene carbonate $\beta \approx 1$. In Table IV we have given a comparison of parameters obtained from our experiment and those from the ac calorimetry[7] for two liquids. While most of the parameters are quite comparable, β determined by us are lower than those obtained in the ac calorimetry. This difference, we believe, reflects the temperature dependence of β. The specific-heat data are most sensitive to τ_s and hence to β when $T \sim T_g$. In our experiment, done at a somewhat longer time scale, the T_g was lower. As a result the β determined by us corresponds to that at somewhat lower temperatures. We then have to conclude that β increases with decreasing temperature in these two materials.[8]

In these experiments we also made one more observation, which we briefly mention here without elaboration. We find that β depends somewhat on the cooling rate[4] and also on the degree of partial crystallization in the supercooled liquid.[13] For glycerol cooled at an average rate of around 0.2 K/min. or less, the β can be as high as 0.7.

We also tried to look at whether there is any correlation of the width of the spectrum of relaxation time measured by β and the glass transition width ΔT_g. For the five different materials studied $\Delta T_g/T_g \simeq 0.18-0.29$, while β can range from 0.45 to 1.0. Thus no definite correlation can be suggested. Determination of ΔT_g, however, becomes somewhat difficult due to the existence of a secondary peak as mentioned earlier.

VI. SUMMARY

The experiment was done with the objective of obtaining the specific-heat data on glass-forming liquids during the cooling process and analyze the data with a model of nonequilibrium cooling so that the relevant parameters regarding the enthalpy relaxation can be obtained and can be compared to the relaxation times measured through other experiments, especially the ac calorimetry.[7,8] This method allows us to do the experiments at longer time scales and thus extend the range of observed relaxation times to lower temperatures. From the analysis of our data we could make a number of interesting observations. We could display the delayed heat release from the unrelaxed enthalpy and the role of this unrelaxed enthalpy in determination of the nonequilibrium relaxation time. We also found that the equilibrium configurational specific heat (C_{FO}) rises as T decreases even down to $T/T_g \approx 0.85$ and the observed fall in the specific heat is entirely relaxational in origin. The temperature T_0, which enters the Vogel-Fulcher law was not found to be a constant, but it decreases, although slightly, as T is decreased, and the relative decrease is the maximum for a fragile liquid. We also found that in a fragile liquid, propylene carbonate, the enthalpy relaxation time

TABLE IV. Comparison of parameters for enthalpy relaxation obtained from a.c. calorimetry and the present investigation (see Eq. 5).

Parameters	Glycerol		Propylene glycol	
	I[a]	II[b]	I[a]	II[b]
A (K)	2500±100	2500±100	2170±100	2020±130
τ_0 (sec)	$(0.2-2)\times10^{-15}$	$(0.03-2)\times10^{-14}$	$(0.15-5)\times10^{-14}$	$(0.63-3.9)\times10^{-14}$
T_0 (K)	128–120	128±5	112–100	114±7
β	0.55±0.02	0.65±0.03	0.45±0.03	0.61±0.04

[a]Obtained in the present investigation.
[b]Obtained from ac calorimetry in Ref. 7.

does not follow the shear relaxation time. But in an intermediate liquid, glycerol, the enthalpy relaxation time matches well with those found by other methods.

We point out that continuous cooling calorimetry alone may not be a sufficient method to give a quantitative estimate of all the relaxational parameters near the glass transition. It should be complemented by other methods such as ac calorimetry or reheating calorimetry (like Differential Scanning Calorimetry), which are done with a well-defined thermal history.

ACKNOWLEDGMENTS

The project was funded by the Department of Science and Technology (Government of India). One of us (M.R.) wants to thank the CSIR for financial support.

[1]M. Rajeswari, S. K. Ramsesha, and A. K. Raychaudhuri, J. Phys. E **21**, 1017 (1988).
[2]R. E. Schwall, R. E. Howard, and G. R. Stewart, Rev. Sci. Instrum. **46**, 1054 (1975), and references cited therein.
[3]B. F. Griffing and S. A. Shivashankar, Rev. Sci. Instrum. **51**, 1030 (1980).
[4]M. Rajeswari, Ph.D. thesis, Indian Institute of Science, 1990.
[5]S. B. Thomas and G. S. Parks, J. Phys. Chem. **35**, 2091 (1931).
[6]O. Sandberg, P. Anderson, and G. Backstron, J. Phys. E. **10**, 474 (1977).
[7]N. O. Birge and S. R. Nagel, Phys. Rev. Lett. **54**, 2674 (1985); N. O. Birge, Phys. Rev. B **34**, 1631 (1986).
[8]P. Dixon and S. R. Nagel, Phys. Rev. Lett. **61**, 341 (1988).
[9]C. T. Moynihan, A. J. Easteal, M. A. deBolt, and J. Tucker, J. Am. Ceram. Soc. **59**, 12 (1976).
[10]P. W. Anderson, in *Ill Condensed Matter,* edited by X. Maynard (North-Holland, Amsterdam, 1979), p. 162.
[11]J. Zimmerman and G. Weber, Phys. Rev. Lett. **46**, 661 (1981).
[12]M. Rajeswari and A. K. Raychaudhuri, Europhys. Lett. **10**, 153 (1989).
[13]M. Rajeswari and A. K. Raychaudhuri (unpublished).
[14]C. A. Angell, J. Phys. Chem. Solids. **49**, 863 (1988).
[15]G. E. Gibson and W. F. Giauque, J. Am. Chem. Soc. **45**, 93 (1923); J. E. Ahilberg, J. Chem. Phys. **5**, 539 (1937).
[16]G. S. Parks and H. M. Huffman, J. Phys. Chem. **31**, 1842 (1927).
[17]S. S. Chang, J. A. Horman, and A. B. Bestul, J. Res. Nat. Bur. Stand., Sect. A **71A**, 293 (1967).
[18]M. Goldstein, J. Chem. Phys. **51**, 3728 (1969).
[19]G. Williams and D. C. Watts, Trans. Faraday Soc. **66**, 80 (1970).
[20]G. Fulcher, J. Am. Ceram. Soc. **8**, 339 (1925).
[21]G. Adam and J. H. Gibbs, J. Chem. Phys. **43**, 139 (1965).
[22]W. Kauzmann, Rev. Mod. Phys. **14**, 12 (1942).
[23]A. Q. Tool, J. Am. Ceram. Soc. **29**, 240 (1946).
[24]O. S. Narayanaswamy, J. Am. Ceram. Soc. **54**, 491 (1971).
[25]S. M. Rekhson, J. Non-Cryst. Solid **73**, 151 (1985).
[26]G. W. Scherer, J. Am. Ceram. Soc. **67**, 504 (1984).
[27]I. M. Hodge, Macromolecules **20**, 2897 (1987).
[28]A. J. Kovacs, Ann. N.Y. Acad. Sci. **371**, 21 (1981).
[29]A. Algeria, J. M. Barandiaran, and J. Colmenero, Phys. Status Solid B **120**, 349 (1983).
[30]J. P. Sethana, J. D. Shore, and M. Huang, Phys. Rev. B **44**, 4943 (1991).
[31]N. Birge, Y. Jeong, and S. R. Nagel, Ann. N.Y. Acad. Sci. **484**, 1001 (1986).
[32]L. Borjesson and W. S. Howells, J. Non-Cryst. Solids **131-133**, 53 (1991).